Indian Journal of Chemistry
Vol. 60A, October 2021, pp. 1303-1308

Elctrocatalytic oxygen evolution reaction on Mg, Al and Fe doped spinel oxides

Basant Lal

Department of Chemistry, Institute of Applied Sciences and Humanities, GLA University, Mathura 281 406, UP, India
*E-mail: basant.lal@gla.ac.in

Received 16 April 2021; revised and accepted 27 September 2021

Metal doped cobalt-based spinel type catalysts prepared by co-precipitation route are considered as suitable candidates for OER, ORR, metal air batteries, fuel cells, detoxification of water, etc. For the purpose, metal doped oxides with formula MCo_2O_4 (M= Mg, Al and Fe) have been prepared by thermal decomposition of their metal carbonate precipitates and characterized by IR, XRD, CV, EIS and Tafel polarization techniques. The FTIR spectra of oxides show absorption bands ~ 650 cm^{-1} and ~ 560 cm^{-1} for respective stretching and bending modes of vibration of Co-O bond at octahedral sites and formation of nano-size (~ 18 nm) single phase cubical crystal with spinel geometry is confirmed by powder XRD patterns. The cyclic voltammetric curves of oxide electrodes in 1 M KOH solution showed a redox peak at E^o = 434 -516 mV for Co^{2+}/Co^{3+} reactions. The electrocatalytic activity of oxide electrodes for oxygen evolution reaction in 1 M KOH at 25 °C was also studied by Tafel polarization technique and polarization curve of each oxides showed two Tafel slopes and order of OER is unity.

Keywords: Doped spinel oxide, Elecrocatalytic oxygen evolution, Tafel slope

World energy demand is increasing rapidly due to exponential growth of world population and rapid industrial development. Presently, maximum requirement of energy is fulfilled by combustion of fossil fuels which has adverse effect on our environment and also emits lot of air pollutants like SO_x, NO_x, CO_2, hydrocarbons etc. into the atmosphere. The increase in CO_2 level in the atmosphere results in global warming and other harmful effects. This has caused great concerns among various communities of the world. It is therefore, desired to supplement at present and substitute in future the conventional energy sources[1]. In the recent years, researches are being carried out to develop economical and efficient technologies to transform inexhaustible renewable energy sources such as solar, wind and water into electricity. Among these energies, the sun light has drowned tremendous interests during recent years[2,3] in relation to its economic conversion for practical purposes.

Spinel (e.g. Co_3O_4, $FeCo_2O_4$, $CuCo_2O_4$, $NiCo_2O_4$, etc.) and perovskite ($LaCoO_3$, $LaMnO_3$, etc.) type of oxides are used as electrode material in electrochemical devices such as water electrolysis cells, fuel cells and metal air batteries[4-11]. Fe-doped cobaltite is used in making high performance super capacitor and electrochemical devices for energy storage[12,13]. Metal-doped oxides were used as catalyst in several electrochemical reactions such as O_2[5-7,14] and Cl_2[15] evolution, O_2 reduction[5,6,16] and also in application to metal ion batteries[8-11]. Hybrid materials comprising of graphene/MCo_2O_4/Pd (where, M = Mn, Co or Ni) used as efficient bi-functional electro-catalysts for oxidation of methanol and reduction of oxygen in fuel cells[11]. Nano-fibre like oxide of $MgCo_2O_4$ obtained by thermal decomposition of their oxalate salts showed reversible capacity, cycling stability and used as anode in Li ion battery[17]. The $NiCo_2O_4$ samples exhibit magnetic properties and high activity and superior cycling stabilities in ORR[18]. Fe and Mg doped cobaltites are synthesized by the urea combustion and oxalate decomposition method, respectively, and characterized by powder XRD, HR-TEM, SAED and XPS. SEM showed the characteristics features in the morphology, submicron-size of $FeCo_2O_4$ and needle-shaped particles of $MgCo_2O_4$[19]. Nano-crystalline $ZnCo_xAl_{2-x}O_4$ (x ¼ 0.00e1.50, step 0.25) oxides were obtained by combustion method using citric acid as precursor and use as a yellow-orange phosphor for displays and/or white light-emitting diodes[20].

The elctrocatalytic efficiency of these oxide materials can be improved by preparing them by newly developed low temperature preparative method. The morphology and hence the electrochemical interfacial properties of the oxide electrode can also be modified by the doping of metal in the oxide metrix. Chi *et al.*[21] synthesized

Ni-Co spinel-type oxides by different routes and investigated the effect of Ni-doping on the physicochemical and electrochemical properties. The lattice parameters, crystallite size and surface composition of the oxide material were investigated by De Faria *et al*.[22]. Recently, Cui *et al*.[23] prepared $NiCo_2O_4$ nano-platelets with core-ring structured by hydroxide co-precipitation decomposition method and characterized their electrocatalytic properties for the OER. In general, it is observed that both electronic and geometrical factors affect the electrocatalytic properties of the material. The former is based on the electronic structure and the nature of the active sites such as Co^{3+} in $NiCo_2O_4$[14], while the latter by the surface concentration of the active sites as well as on actual surface area[22]. This investigation, focuses on synthesis of cobalt based metal doped spinel oxides with improved electrocatalytic properties by carbonate co-precipitation method and studied the effect of doping of different metal in oxide lattice on the physicochemical and electrochemical properties mainly for O_2 evolution (OE) reaction in 1 M KOH solution.

Materials and Methods

$MgCo_2O_4$, $AlCo_2O_4$ and $FeCo_2O_4$ were used in electrocatalysis of OE have also been prepared by using their metal salts, particularly metal nitrates as precursors. The nitrate salts of metals of analytical grade were dissolved in double distilled water as per their stoichiometric requirements in the oxide and then metal ions are precipitated as metal carbonates by adding Na_2CO_3 solution at 60 °C.[24] The resultant metal carbonate precipitate was filtered and washed thoroughly by double distilled water, dried at 120 °C for 12 h and heated in electrical furnace at 350 °C for 4 h in presence of air to obtained spinel oxide. The materials were characterized by infrared (IR) spectra (JASCO FT/IR-5300) and powder XRD techinque (Co-K_α-radiation, $\lambda = 0.178889$ nm).

For electrochemical investigation, adherent oxide film on pre-treated nickel support was obtained by oxide-slurry painting method. In this method, the required amount of oxide powder was placed in Agate pestle mortar and ground continuously for half an hour with few drops of glycerol as binder. The slurry so prepared, was coated onto on one side of nickel plate (geometrical surface area: 1.5 cm ×1 cm, Aldrich 99.9% purity) with the help of fine brush, dried and then heated in an electronically controlled furnace for 1 h at 350 ± 10 °C. For good adherent film, plate was removed from furnace when it attained at temperature <100 °C. This procedure was repeated to obtain the oxide of desired loading. The procedure adopted for the pre-treatment of nickel support and electrical contact is similar to those reported in literature[25,26].

The electrochemical cell used in this experiment consists of electrolyte, counter electrode (Pt-foil with area 12.3 cm^2, Aldrich 99.9% purity) and reference electrode (Hg/HgO/1M KOH). Instruments used for electrochemical characterizations as well as methodology followed in cyclic voltammetry, electrochemical impedance and Tafel polarization studies were almost similar to those reported in literature[26]. In each experiment, reference electrode is separated from test solution by using luggin capillary containing aqueous agar-agar (KCl) salt bridge. All the potential values reported in the text correspond to the reversible potential for the reference electrode Hg/HgO/1 M KOH (98 mV vs NHE) only. The instrument used in the investigation was the electrochemical impedance system (EG & G, PARC, USA) comprising with lock-in-amplifier (model 5210), and potentio-galvanostat (model 273A).

Results and Discussion

Material Characterisation

Formation of pure and crystalline spinel oxides was confirmed by IR spectroscopy and powder XRD patterns. IR-spectra of metal-substituted oxides (Fig. 1) show peaks at 650 and 560 cm^{-1} ascribed to characteristic stretching and bending modes of vibrations of Co-O bond in octahedral site[25,26], respectively, and peak at ~3450 cm^{-1} correspond to M-OH vibration. Peaks at 3000-3150 cm^{-1} and 1630 cm^{-1} are due to O-H and H-O-H oscillations and this confirms the presence of water.

Powder XRD patterns of $MgCo_2O_4$, $AlCo_2O_4$ and $FeCo_2O_4$ are shown in Fig. 2. This figure shows the oxides are crystalline, nano-sized spinel with cubic crystal geometry ($a = b = c$ and $\alpha = \beta = \gamma = 90°$). The crystallographic density (d) was estimated using the relation, d = 8 M/V, where M and V are corresponding molecular mass and volume of the compound assuming 8 molecules of oxide in a unit cell. The computed values of cubic cell parameter are ~8.072 Å, ~8.085 Å, and~8.14 Å, for $MgCo_2O_4$, $AlCo_2O_4$, and $FeCo_2O$, respectively. These values of lattice parameters are very close to their literature values, for example, $MgCo_2O_4$ 8.123 (JCPDS # 02-1073) and 8.086 (Ref.27).

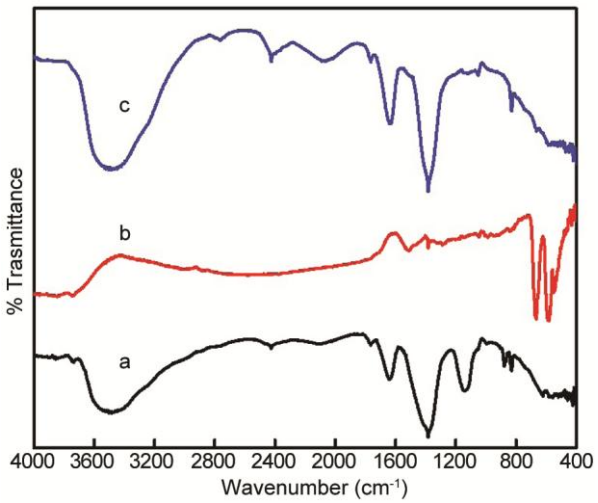

Fig. 1 — FTIR spectra of oxide (a) $MgCo_2O_4$ (b) $AlCo_2O_4$ and (c) $FeCo_2O_4$ prepared at 350 °C for 5 h

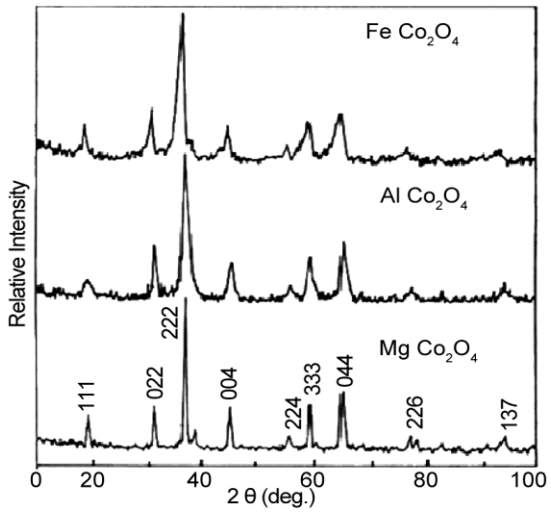

Fig. 2 — Powder XRD patterns of oxides prepared at 350 °C for 5 h

The unit cell parameters of cobalt based oxides are given in Table 1. Metal doping marginally affect the value of lattice parameter '*a*' while slight increase in *a*-value observed in $FeCo_2O_4$, similar increase in *a*-value was also been reported in literature[25,28] wherein oxides were obtained by other methods. The crystallite size (S) of the oxide was calculated by Schrrer's formula, $S = 0.9\ \lambda / \beta \cos\theta$, where λ is the wavelength of radiation, β is full width at half maximum of the most intense peak in radian and θ is corresponding angle in degree. The calculated value of crystal dimensions were 18.1 nm, 33.1 nm and 19.8 nm for $AlCo_2O_4$, $MgCo_2O_4$ and $FeCo_2O_4$, respectively. The results show that carbonate co-precipitation produces nano-sized single phase spinel oxides with comparatively smaller size than those obtained by oxalic acid precipitation method[29], however, larger than those of prepared by ethanol evaporation method. Al and Fe substituted oxides show half of size than that of Co_3O_4 (Ref. 25).

Table 1 — Unit cell parameters of oxides at 350 °C

Oxide	*a* (Å)	V $(Å)^3$	*d* (g cm^{-3})	S (nm)
$AlCo_2O_4$	8.085	528.49	5.249	18.1
$MgCo_2O_4$	8.072	525.95	5.207	33.1
$FeCo_2O_4$	8.14	539.35	5.853	19.8

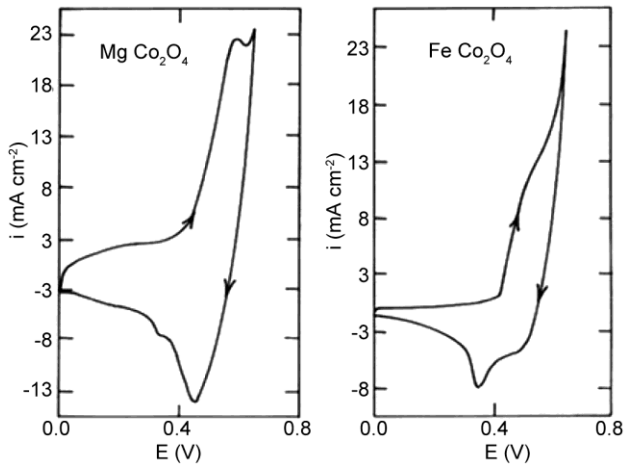

Fig. 3 — Cyclic voltammograms of $MgCo_2O_4$ and $FeCo_2O_4$ films on nickel at 20 mV s^{-1} in 1 M KOH (25 °C)

Cyclic voltammetry (CV)

In order to know the redox behaviour of the oxide/solution interface, cyclic voltammetry of each oxide were recorded in 1 M KOH at 25 °C over the potential range of 0.0 to 650 mV at the scan rate of 20 mV/sec at 25 °C. Two representative cyclic voltammetric curves of $MgCo_2O_4$ and $FeCo_2O_4$ are given in Fig. 3. Cyclic voltamogram of oxide electrodes shows a pair of redox peaks corresponding to anodic and cathodic reactions. The values of peak potentials E_{pa}, $E_{pc,}$ and the formal redox potential ($E^0 = E_{pa} + E_{pc}/2$) were analyzed and are listed in Table 2.

Cyclic voltammetric curves shows that E^0-value for oxide electrodes are ranges 416 – 534 mV corresponding to the redox reaction $Co(IV) + e^- \leftrightharpoons Co(III)$[31]. Al-doped cobaltite matrix reduces the E^0-value while Mg and Fe doped cobaltites shows more or less similar nature as in pure cobaltite[25]. Cyclic voltamogram of $FeCo_2O_4$ shows more reversible nature due to the lower difference in their peak potentials.

Table 2 — CV parameters for oxide electrodes in 1 M KOH at 20 mV s^{-1} (25 °C)

Electrode	E_{pa} (mV)	E_{pc} (mV)	ΔE_p(mV)	E_p^0 (mV)
$AlCo_2O_4$	494	338	156	416
$MgCo_2O_4$	593	457	136	525
$FeCo_2O_4$	570	498	72	534

Impedance spectroscopy/Roughness factor (R_F)

For the determination of double layer capacitance (C_{dl}) of the catalyst/1 M KOH interface, impedance spectra of oxide electrodes were recorded in the frequency range from 0.1 to 10^5 Hz at three different potentials 0, 50 and 100 mV in 1 M KOH at 25 °C. In this region of DC potentials effect of charge transfer process is very low as it is supported by cyclic voltammogram shown in Fig. 3. The C_{dl} of the catalyst/ 1 M KOH interface was determined by analysing impedance data using series Rs(RQ) (RQ)(RC) equivalent circuit model[32], where L, R, Q and C are the inductance (henri), resistance (ohm), constant phase element (FS^{n-1}) and capacitance (farad), respectively. The series model is fairly reproducing the feature of experimental curves. Impedance spectra of $AlCo_2O_4$ and $FeCo_2O_4$ in both Nyquist and Bode forms at 50 mV in 1 M KOH are shown in Fig. 4 (a & b). The values of oxide roughness factor was estimated from the C_{dl} value of the oxide/solution interface assuming 60 $\mu F cm^{-2}$ as the C_{dl} for smooth oxide surface[4,15,33]. The value of C_{dl} and other circuit parameters determined at three DC potentials were approximately the same and their average values are given in Table 3.

The doping of metals (viz. Fe, Al & Mg) in Co_3O_4 matrix reduces the oxide roughness factor (~47 times in $FeCo_2O_4$, ~28 times in $AlCo_2O_4$ and ~ 2.4 in $MgCo_2O_4$) [(Ref. 25)]. Similar reduction in oxide roughness factor was also reported in literature[33]. It is noteworthy that the roughness factor for Mg, Al and Fe doped oxides produced by this method is considerably lower than those reported for Co_3O_4 film[25]. For example, the Co_3O_4 films on Ni, Ti, and Cd/glass prepared by spraying[34] and on Ni prepared by sequential solution coating[21] and hydroxide co-precipitation method[35] were ~530, ~9, and ~63, respectively. It is worth mentioning that the RF values quoted in the literature were determined by cyclic voltammetry.

Electrocatalytic Activity

The electrocatalytic activities of metal-doped Co_3O_4 have been examined with respect to the electrolytic oxygen evolution reaction (OER) in 1 M KOH at 25 °C. For the purpose, the anodic polarization curves were recorded on each oxide catalyst in 1 M KOH at the scan rate of 0.2 mV sec^{-1}. The values of Tafel slope at two potentials, low (b_1) and high (b_2) corresponding to each polarization curves were estimated and are given in Table 4. To compare the electrocatalytic activity of catalysts, the apparent current density (i_a) and true current density (i_t) at two potentials 650 and 700 mV were determined from polarization curves are given in Table 4. It is observed that i_a value at both potentials decreases with metal-substitution in cobaltite matrix[25]. Maximum reduction (more than 3 times) observed in case Al-doping. However, Mg and Fe substitution show ~2 times reduction in apparent current density. The reduction in values of apparent current densities may due to change in electronic nature as well as lower oxide roughness factor.

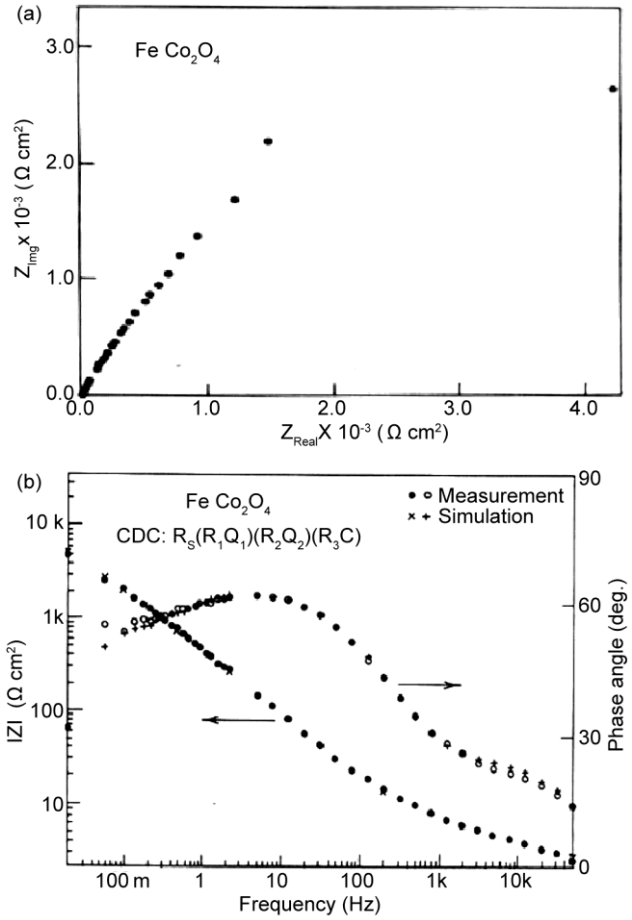

Fig. 4 — (a) Complex impedance (Nyquist) plots for $AlCo_2O_4$ and $FeCo_2O_4$ electrodes in 1M KOH at E = 50 mV (25 °C). and (b) Bode plots for $FeCo_2O_4$ electrodes in 1 M KOH at E = 50 mV (25 °C)

The order of reaction (p) for oxygen evolution reaction was determined by performing anodic Tafel polarization study on metal oxide electrodes at

Table 3 — Equivalent circuit parameters for OER on oxide electrodes in 1M KOH at 25 °C

Electrode	Loading (mg cm^{-2})	R_1 (ohm)	R_2 (ohm)	$Q_1 \times 10^5$ (Fs^{n-1})	n	$R_3 \times 10^{-3}$ (ohm)	$Q_2 \times 10^3$ (Fs^{n-1})	n	$R_4 \times 10^{-3}$ (ohm)	C x 10^{-3} (mF)	R_f
$AlCo_2O_4$	4.9	2.46	1	4.92	0.9	2.07	77.9	0.69	5.07	2.23	37
$MgCo_2O_4$	4.8	4.13	28.4	27.1	0.61	0.09	0.77	0.63	1.66	25.7	429
$FeCo_2O_4$	5.2	2.08	4.1	37.9	0.63	1.58	66.7	0.7	5.17	1.13	22

Table 4 — Electrode kinetic parameters for OER on oxide electrodes in 1M KOH at 25 °C

Electrode	Loading (mg cm^{-2})	Tafel slope (mV $decade^{-1}$)		Order (p)	i (mA) cm^{-2} at E/mV			
					650		700	
		b_1	b_2		i_a	$i_t \times 10^2$	i_a	$i_t \times 10^2$
$AlCo_2O_4$	4.9	69	117	1.3	2.6	7	46.2	124.8
$MgCo_2O_4$	4.4	60	103	1.2	4.7	11	119	27.7
$FeCo_2O_4$	5.2	55	89	1.2	4.3	19.5	135.8	617.3

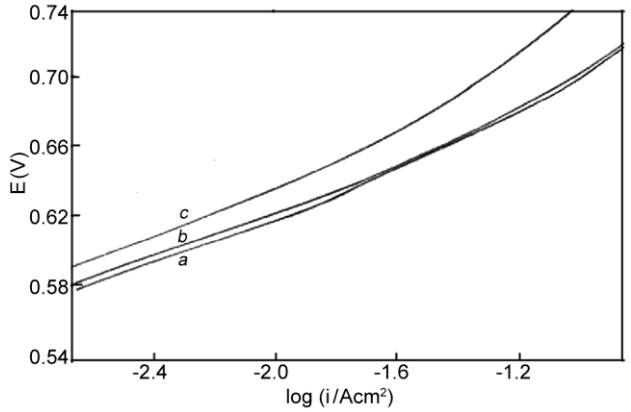

Fig. 5 — iR-free Tafel polarization plots on cobaltite films on Ni in 1 M KOH at 25 °C: (a) $MgCo_2O_4$ (b) $FeCo_2O_4$ and (c) $AlCo_2O_4$

different KOH concentrations at constant ionic strength (μ) of the medium using inert electrolyte (KNO_3) and temperature. The order of OER in all oxides was found to be approximately unity. Tafel polarization curves (Fig. 5) show two Tafel regions, one at low potential (b_1) and other at higher potential (b_2). The b_1 values for OER on different catalysts ranged between 55 and 69 mV $decade^{-1}$ and b_2 values, 89 and 117 mV $decade^{-1}$ and order for OER on different catalysts is approximately unit suggest that the electro-formation of oxygen on the oxide catalysts follows almost similar mechanism, regardless of the metal-substitution in Co_3O_4 matrix[35].

Conclusions

The results showed that co-precipitation method is simple and economical for the production of single phase nano-sized spinel type oxides that can be used in several applications such as in electro-formation of O_2, Cl_2, metal air batteries etc. Electrocatalytic study showed Al and Fe doping reduce oxide roughness factor. $FeCo_2O_4$ electrode found to be stable and electrocatalytically more active for OER in alkaline medium and showed more reversible nature towards redox reaction for oxygen evolution. However, all oxide electrodes follow similar reaction mechanism with unit order and two Tafel slopes (b_1 and b_2) at low and high potential regions, respectively.

Acknowledgement

The author owes the debt of gratitude to Prof R. N. Singh of Department of Chemistry, Banaras Hindu University Varanasi, for providing required facilities to carry out this investigation.

References

1 Bockris J O and Reddy A K N, *Electrodics in Chemistry, Engineering, Biology and Environmental Science* in *Modern Electrochemistry* Vol 2B, Second Edition (Kluver Academic Planum Publishers, New York) 1998.
2 Koval C A & Honeard J N, *Chem Rev*, 92 (1992) 411.
3 Bard J L, *J Phys Chem*, 86 (1982) 172.
4 Singh R N, Koenig J F, Poillerat G & Chartier P, *J Electrochem Soc*, 137 (1990) 1408.
5 Wang Y, Liu Q, Hu T, Zhang L & Deng Y, *Appl Surf Sci*, 403 (2017) 51.
6 Wang Y, Liu Q, Zhang L, Hu T, Liu W, Liu N, Du F, Li Q & Wang Y, *Int J Hydrog Energy*, 41 (2016) 22547.
7 Yan W, Cao X, Tian J, Jin C, Ke K & Yang R, *Carbon*, 99 (2016) 195.
8 Zhang Z, Li W, Zou R, Kang W, San Chui Y, Yuen M F, Lee C S & Zhang W, *J Mater Chem A*, 3 (2015) 6990.
9 Wang B, Li S, Wu X, Li B, Liu J & Yu M, *Phys Chem Chem Phys*, 17 (2015) 21476.
10 Zhang X, Xie Y, Sun Y, Zhang Q, Zhu Q, Hou D, & Guo J, *RSC Adv*, 5 (2015) 29837.
11 Mao J, Hou X, Wang X, Hu S & Xiang L, *Mater Lett*, 161 (2015) 652.
12 Xu G, Zhang Z, Qi X, Ren X, Liu S, Chen Q, Huang Z & Zhong J, *Ceramic Int*, 44 (2018) 120.
13 Mohmed S G, Attia S Y & Hassan H H, *Micro Meso Mater*, 251 (2017) 26.

14 Marsan B, Fradette N, & Beaudoin G, *J Electrochem Soc*, 139 (1992) 1889.
15 Boggio R, Carugati A, Lodi G & Trasatti S, *J Appl Electrochem*, 15 (1985) 335.
16 Singh R N, Koenig J F, Poillerat G & Chartier P, *J Electroanal Chem Interf Electrochem*, 314 (1991) 241.
17 Darbar D, Reddy M V, Sundarrajan S, Pattabiraman R, Ramakrishna S, & Chowdari B V R, *Mater Res Bull*, 73 (2016) 369.
18 Liu Z Q, Xiao K, ZhiXu Q, Li N, Su Y Z, Wanga H J & Chen S, *RSC Advances*, 3 (2013) 4372.
19 Sharma Y, Sharma N, Rao G V S & Chowdari B V R, *Solid State Ion*, 179 (2008) 587.
20 Wahba A M, Imam N G & Mohamed M B, *J Mol Struct*, 1105 (2016) 61.
21 Chi B, Li J B, Han Y S & Dai J H, *Mater Lett*, 58 (2004) 1415.
22 Faria L A D, Prestat M, Koenig J F, Chartier P & Trasatti S, *Electrochim Acta*, 44 (1998) 1481.
23 Cui B, Lin H, Li J B, Li X, Yang J & Tao J, *Adv Funct Mater*, 18 (2008) 1440.
24 Li G H, Dai L Z, Lu D S & Peng S Y, *J Solid State Chem*, 89 (1990) 167.
25 Lal B, Singh R N & Singh N K, *J New Mat Electrochem Systems*, 21 (2018) 163.
26 Singh N K, Tiwari S K, Anitha K L & Singh R N, *J Chem Soc Faraday Trans*, 92 (1996) 2397.
27 Krishnan S G, Reddy M V, Harilal M, Vidyadharan B, Misnon I I, Rahim M H A, Ismail J & Jose R, *Electrochem Acta*, 161 (2015) 312.
28 Zhu H, Sun Y, Zhang X, Tang L & Guo J, *Mater Lett*, 166 (2016) 1.
29 Ferreira T A S, Waerenborgh J C, Mendonç M H R M, Nunes M R & Costa F M, *Solid State Sci*, 5 (2003) 383.
30 Chang S K, Zainal Z, Tan K B, Yusof N A, Yusof W M D W & Prabhakaran S R S, *Sains Malaysiana*, 41 (2012) 465.
31 Baggio R, Carugati A & Trasatti S, *J Appl Electrochem*, 17 (1987) 828.
32 Boukamp B A, *Solid State Ion*, 20 (1986) 31.
33 Levine S & Smith A L, *Discuss Faraday Soc*, 52 (1971) 290.
34 Hamdani M, Koenig J F & Chartier P, *J Appl Electrochem*, 18 (1988) 568.
35 Godinho M I, Catarinno M A, Pereira M I D S, Mendonca M H & Costa F M, *Electrochim Acta*, 47 (2002) 4307.